Reduction of High-frequency Vibration Noise for Dual-branch Three-phase Permanent Magnet Synchronous Motors*

Wentao Zhang[1], *Yongxiang Xu*[1*], *Yingliang Huang*[2] *and Jibin Zou*[1]

(1. School of Electrical Engineering and Automation, Harbin Institute of Technology, Harbin 150001, China;
2. Automotive-Products-Group, Johnson Electric, Shenzhen 518125, China)

Abstract: Two-level voltage source inverters with pulse width modulation (PWM) generate multiple carrier harmonics, thereby exciting high-frequency noise from the motor. Based on a special dual-branch three-phase permanent magnet synchronous motor (PMSM), a method that utilizes a known modified space vector PWM technique is proposed. This method is able to suppress unpleasant high-frequency vibration noise as well as acoustic noise more effectively than other methods. Vibration noise near the twice carrier frequency is eliminated, and PWM vibration noise around the carrier frequency is also reduced. In particular, vibration and acoustic noise at the twice carrier frequency are eliminated using a carrier phase-shift of 0.5π and the special winding structure of the dual-branch PMSM. The effectiveness of the proposed method is confirmed using detailed experimental results.

Keywords: Motor drives, permanent magnet synchronous motor (PMSM), pulse width modulation (PWM), vibration

1 Introduction

Permanent magnet synchronous motors (PMSMs) are widely utilized for various applications and in various devices, such as electric vehicles, electric ship propulsion, aircraft, robotics, and space exploration[1]. Multi-phase permanent magnet motors are becoming more popular because of their higher torque densities, enhanced efficiency, and fault-tolerant capabilities[2-3]. Many studies have been conducted on multi-phase motor topologies, design, and control methods, owing to which dual three-phase PMSMs have attracted significant attention[3-5]. The dual three-phase PMSM is usually driven by two paralleled two-level voltage source inverters (VSIs) owing to its simple structure and mature control strategy[6]. Space vector pulse width modulation (SVPWM) is widely employed in voltage source inverters to achieve excellent static and dynamic performance. However, unpleasant acoustic switching noise is generated by undesirable high-frequency pulse width modulation (PWM) voltage and current harmonic noise near the carrier frequency (and its multiples) during the intrinsic switching process[7]. The switching frequency is selected between 2 kHz and 20 kHz (within the human hearing range) to reduce switching losses. Thus, it is necessary to address this problem for the sake of comfort.

From the perspective of a power device, the emerging wide bandgap power devices, including silicon carbide and gallium nitride, exhibit advantages over conventional silicon such as higher breakdown voltage with lower on-resistance and faster switching speed[8-10]. Nevertheless, cost and current limitations are obstacles that prevent them from being widely applied. With regards to the control strategy, carrier phase-shift (also called the interleaving technique) and improved SVPWM have been proposed to reduce PWM harmonics[11-13].

For dual three-phase PMSMs with two three-phase windings shifted by $\pi/6$ driven by paralleled inverters, the results in Ref. [14] reveal that vibration and sound pressure can be approximately halved near the twice carrier frequency when the carrier phase is $\pi/2$ rad between each VSIs compared to conventional in-phase carrier PWMs. However, the resulting current harmonics caused by carrier phase

Manuscript received February 23, 2020; revised March 24, 2020; accepted April 15, 2020. Date of publication June 30, 2020; date of current version April 27, 2020.

* Corresponding Author, Email: xuyx@hit.edu.cn

* Supported by the National Natural Science Foundation of China (51577036, 51437004).

Digital Object Identifier: 10.23919/CJEE.2020.000010

-shift remain a serious problem. Shifting carrier phase by $\pi/2$ for two-segment three-phase PMSMs driven by interleaved paralleled VSIs without coupled inductors can largely reduce torque ripple in terms of even-order carrier frequency. However, it has almost no effect on the reduction of vibration noise[5]. And adding coupled inductors(CIs) with carrier phase shifted by π also has an impact on noise reduction of odd-order carrier frequency harmonics because of decreasing current harmonics, whereas the noise nearby odd-order carrier frequency is not eliminated completely and even-order carrier frequency noise is not influenced[15]. For the dual-branch three-phase PMSM in Ref. [16], using a carrier phase shift of π and highly-coupled inductors can completely eliminate the odd-order carrier frequency harmonics, but even-order carrier frequency harmonics still exist and are not affected.

Random PWM (RPWM) techniques to reduce voltage and acoustic noise have been researched in detail. RPWM-based methods spread the power of noise over a wide range of frequency domains, and the peak of PWM noise in phase voltage is decreased by 9-10 dB[17-19]. Random switching frequency PWM, as one of the RPWM techniques, achieves good voltage and current harmonic elimination at both low and high speed[18]. A shorter random frequency range will weaken the effect of RPWM. Thus, in many situations, RPWM cannot satisfy the demand for low noise. Moreover, the increase in background noise and incomplete reduction of PWM harmonic noise require further study. Modified SVPWM (MSVPWM), which is introduced in Ref. [20], exchanges the active vector in the next half of the PWM period and reduces the odd carrier frequency harmonics at the cost of slightly increasing the switching losses. Combining the modified SVPWM and other techniques can also further reduce all multiples of carrier frequency noise[21]. However, the carrier and twice carrier frequency vibration noise has only been reduced in recent research, and especially, the elimination of twice carrier frequency noise has not been accomplished. Therefore, the total elimination of twice carrier frequency noise for dual three-phase PMSMs should be studied further.

This paper extends the work in Ref. [16] and further eliminates the twice carrier frequency noise on the dual-branch three-phase PMSM driven by paralleled three-phase VSIs with the carrier phase-shift technique, as shown in Fig. 1. The total elimination of the twice carrier frequency is mainly dependent on the special structure of the motor rather than the coupled inductors, with which identical noise elimination cannot be achieved for other types of dual three-phase PMSMs driven by the same topology. With the proposed method, the acoustic noise under 20.0 kHz can, therefore, be reduced to a considerable extent when the switching frequency is selected as 4.0 kHz. Although the drive system has coupled inductors, the dynamics and reliability of the system are not influenced due to its structure[22-23]. The research provides a method for dual-branch three-phase PMSM and significantly reduces the acoustic noise, and it can be used in other paralleled interleaving topologies.

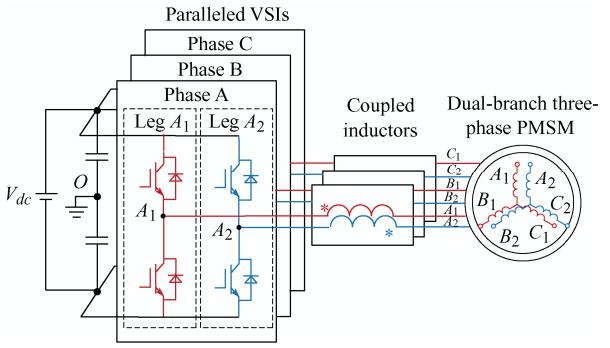

Fig. 1 Drive system for dual-branch three-phase PMSM with carrier phase-shift

The rest of this paper is organized as follows. Section 2 reviews the modified SVPWM and introduces the implementation of the proposed method for the reduction of high-frequency PWM vibration. The vibration elimination principle of carrier frequency and twice carrier frequency harmonics is elaborated in Section 3. Experiments are carried out on the dual-branch three-phase PMSM using the digital signal processor control board in Section 4. Finally, conclusions are presented in Section 5.

2 Introduction of the proposed method

2.1 Review of the modified SVPWM

Traditional seven-segment regular sampled SVPWM generates high-frequency harmonics near the carrier frequency and its multiples. To reduce ear-piercing acoustic noise for odd-order carrier frequency, a novel MSVPWM is applied.

As shown in Fig. 2, in one PWM cycle, the vector

sequence in sector I is V_0, V_1, V_2, V_7, V_1, V_2, V_0 instead of V_0, V_1, V_2, V_7, V_2, V_1, V_0. In other sectors, the sequence of the active vector in the second half PWM period should be alternated. From the phase voltage of the A-phase, it can be observed that the phase voltage wave is not symmetric for V_7 as the dotted line but has a period of $0.5T_c$. Although the sequence of the active vector is changed, the duty cycle for one PWM interval remains constant.

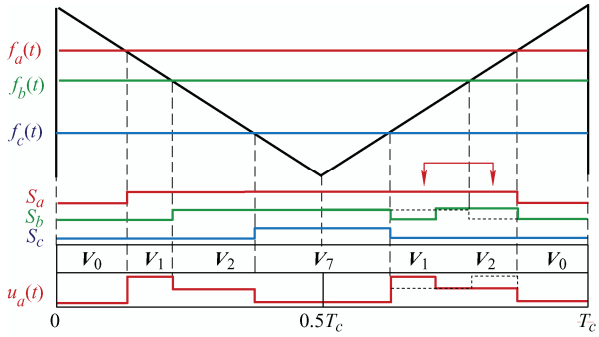

Fig. 2 Schematic of the MSVPWM

2.2 Implementation of the proposed method

The proposed method combines the modified SVPWM and carrier phase-shift of 0.5π to lower the high-frequency noise of dual-branch three-phase PMSMs comprehensively, with the aid of the special winding structure. The method for its implementation is simple. Fig. 3 demonstrates the PWM generation process for sector I, from which it can be observed that the PWM for the two inverters has the 0.25 PWM period phase-shift and an identical duty ratio in one PWM cycle to maintain the synchronous fundamental current.

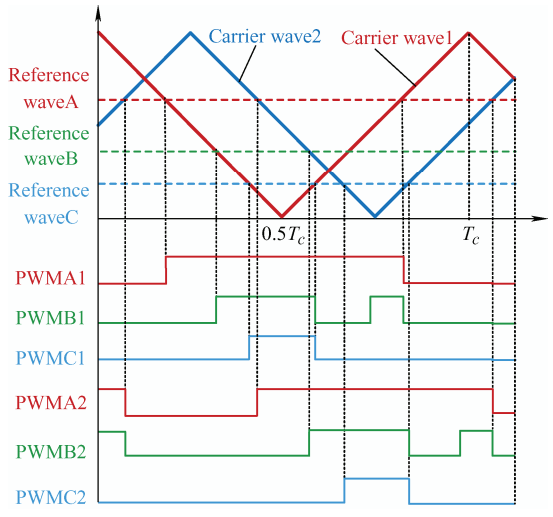

Fig. 3 PWM generation wave for the proposed method

3 Principle of vibration elimination

First, the elimination of the high-frequency PWM current harmonics is analyzed by equivalent circuits, and then the corresponding reduction principle of vibration noise is introduced in this section.

3.1 Analysis of PWM current harmonics

The PWM current harmonics in dual-branch three-phase motor driven by paralleled VSIs with CIs using the proposed method are discussed in this part.

The phase voltage harmonics using conventional SVPWM for the three-phase VSIs can be simplified as[24]

$$u_h(t)=\sum_{m=1}^{\infty}\sum_{n=-\infty}^{\infty}C_{mn}\cos(m(\omega_c t+\varphi_c)\pm n(\omega_0 t+\theta_0)) \quad (1)$$

where C_{mn} represents the magnitude of high-frequency carrier and its sideband harmonics. ω_0 and ω_c are the angular frequency of the fundamental wave and carrier wave, respectively. θ_0 and φ_c are the offset phase of fundamental waves and carrier wave, respectively. m and n are integers with opposite parity. The high-frequency harmonics concentrate near $m\omega_c \pm n\omega_0$.

In contrast, the expression of phase voltage harmonics using MSVPWM consists of two parts: one part contains no odd-order carrier harmonics for the former half carrier period, and the other covers odd-order carrier harmonics for the latter half carrier period[25]. Therefore, the PWM voltage of MSVPWM can be simplified as

$$u_h(t)=\sum_{m=1}^{\infty}\sum_{n=-\infty}^{\infty}A_{mn}\cos(m(\omega_c t+\varphi_c)\pm n(\omega_0 t+\theta_0)) \quad (2)$$

where A_{mn} is smaller than conventional SVPWM when m is an odd number, for which the odd multiples of carrier frequency voltage harmonics are reduced. Furthermore, A_{mn} is equal to C_{mn} when m are even numbers. Hence, only the current harmonics near odd carrier frequency are decreased.

When $\varphi_c=0.5\pi$ for the carrier wave of the second VSIs, the harmonic phase voltage A at twice carrier frequency when m=2 for the two VSIs can be expressed from Eq. (2) as

$$u_{a1h}(t)=\sum_{n=-\infty}^{\infty}A_{2n}\cos\left[2(\omega_c t+0)\pm n(\omega_0 t+\theta_0)\right] \quad (3)$$

$$u_{a2h}(t)=\sum_{n=-\infty}^{\infty}A_{2n}\cos\left[2(\omega_c t+0.5\pi)\pm n(\omega_0 t+\theta_0)\right] \quad (4)$$

From the two equations, $u_{a1h}(t)=-u_{a2h}(t)$.

Fig. 4 shows the equivalent circuits for the twice carrier frequency harmonics. L_c and R_c are the self-inductance and resistance of the coupled inductor, respectively. L_s and R_s are the self-inductance and resistance of the dual-branch PMSM, respectively.

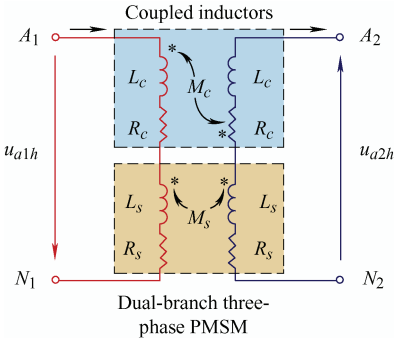

Fig. 4 Equivalent circuit for twice carrier frequency current harmonics

From the symmetric equivalent circuit in Fig. 4, magnitude and phase of the harmonic impedance in one branch for twice carrier frequency current harmonics can be expressed as

$$|z_h|=\sqrt{\omega^2(L_s+L_c+M_c-M_s)^2+(R_c+R_s)^2} \quad (5)$$

$$\angle z_h=\arctan\frac{\omega(L_s+L_c+M_c-M_s)}{R_c+R_s} \quad (6)$$

where $\omega=2\omega_c\pm n\omega_0$. Moreover, as $u_{a1h}(t)=-u_{a2h}(t)$, the two current harmonics are identical apart from the phase. Then, the summation of the twice carrier frequency current harmonics is equal to zero. It should be noted that the subtraction of L_s and M_s in Eq. (5) is not large enough. Hence, a coupled inductor is added to block the harmonics.

From the above analysis, the proposed method can effectively suppress the carrier frequency current harmonics and eliminate the twice carrier frequency harmonics of the summation of the two branches.

3.2 Elimination principle of vibration

Electromagnetic vibration noise is mainly caused by radial electromagnetic forces, and based on the Maxwell tensor method, the radial electromagnetic force, p_r, of the three-phase PMSM can be expressed as[26-27]

$$p_r\approx\frac{[f_M(\theta,t)+f_A(\theta,t)]^2\Lambda^2(\theta)}{2\mu_0} \quad (7)$$

where $f_M(\theta,t)$ is the magneto motive force (MMF) generated by the slotless radial permanent magnet field, and $f_A(\theta,t)$ is produced by the slotless radial armature reaction field. The effect of stator slotting on the air-gap field can be analyzed through a relative permeance function. $\Lambda(\theta)$ is the real part of the relative permeance, μ_0 is the vacuum permeability, and θ is the angular position. As this study only focuses on the time harmonics rather than both spatial and time harmonics, then Eq. (7) can be simplified as Eq. (8) by seeing the θ as a constant.

$$p_r\approx\frac{[f_M(t)+f_A(t)]^2\Lambda^2}{2\mu_0} \quad (8)$$

Moreover, the $f_M(t)$ and $f_A(t)$ can be written as the product of turns N and current $i(t)$ in Eqs. (9) and (10), respectively.

$$f_M(t)=N_M i_1(t) \quad (9)$$

$$f_A(t)=N_A i_h(t) \quad (10)$$

where $i_1(t)$ is the fundamental current, and $i_h(t)$ is the harmonic current. N_M and N_A are the equivalent turns, respectively. Substituting the two equations into Eq. (8) simplifies it as

$$p_r\approx\underbrace{\frac{N_M^2 i_1^2(t)\Lambda^2}{2\mu_0}}_{\text{Part 1}}+\underbrace{\frac{2N_M N_A i_1(t) i_h(t)\Lambda^2}{2\mu_0}+\frac{N_A^2 i_h^2(t)\Lambda^2}{2\mu_0}}_{\text{Part 2}} \quad (11)$$

It should be noted that the force produced by the armature reaction field itself, as shown in Part 2 in Eq. (11), can be neglected owing to its small amplitude, and therefore, Part 1 plays a dominant role in high-frequency vibration. For the proposed motor, the sum of current harmonics in the two three-phase wingdings reflects the high-frequency vibration. Once the sum of current harmonics in $i_h(t)$ with the frequency of $mf_c\pm nf_1$ is eliminated, the corresponding vibration with the frequency of $mf_c\pm(n\pm1)f_1$ is also suppressed[26]. f_c and f_1 are the carrier frequency and fundamental frequency, respectively.

To be more explicit, Fig. 5 illustrates the harmonic MMF $f_{A\_1}(t)$ near carrier frequency and $f_{A\_2}(t)$ near twice carrier frequency produced by the sum of

current harmonics, $i_{h\_1}(t)$ and $i_{h\_2}(t)$, in the two coils with no phase-shift SVPWM and the proposed method. In contrast, in Fig. 5b, the hybrid method decreases the peak of the MMF harmonics by suppressing the carrier frequency harmonics $i_{h\_1}(t)$ and eliminates the twice carrier frequency MMF harmonics, because the sum of current harmonics $i_{h\_2}(t)$ is zero. For the entire motor, the same effects can be achieved, as the spatial and time variable for the two windings are identical. Therefore, the proposed method can effectively suppress vibration of the dual-branch three-phase motor.

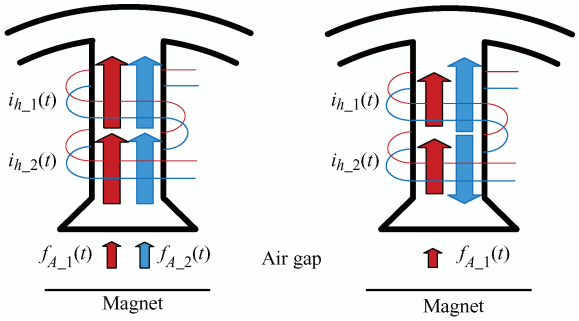

(a) No phase-shift conventional SVPWM (b) Proposed method

Fig. 5 Carrier frequency and twice carrier frequency MMF produced by carrier frequency and twice carrier frequency harmonics near one tooth in the air-gap

4 Experimental validation

This section describes the process by which a PMSM drive system is implemented to verify the capability of PWM noise reduction with the combined method practically. The experiment platform based on MCU C2000 from Texas Instrument is set up to validate the above analysis, and the test bench is shown in Fig. 6. Vibration sensors are glued on the motor surface to measure the high-frequency vibration. As the experiments are conducted to confirm the reduction of the high-frequency harmonic spectrum, the Brüel & Kjær® 2250S noise analyzer is used to measure acoustic noise from motor at a distance of 10 cm. In addition, the coupled inductors are made by 'EC' ferrite cores. The hysteresis dynamometer loads the motor. The specification and parameters of the drive system are listed in Tab. 1.

The PWM current harmonics, vibration, and acoustic noise are compared with the method of traditional SVPWM, MSVPWM, and the proposed method to demonstrate the advantages in removing PWM noise. The motor is tested at low (0.25), medium (0.5), and high (0.85) modulation ratios for paralleled inverters.

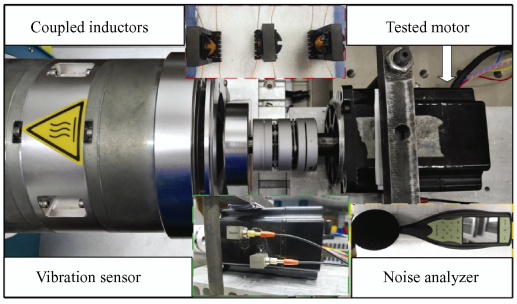

Fig. 6 Text bench

Tab. 1 Systems parameters

Parameter	Value
Switching frequency/kHz	4
Phase inductance/mH	2.3
Phase resistance/Ω	1.8
DC-side input voltage/V	50
Phase current/A	1.5
Rotor speed/(r/min)	960
Torque/(N • m)	1.2
Pole pairs	5
Inductance of CI/mH	4.9
Resistance of CI/Ω	0.1

4.1 Results for PWM current harmonics reduction

For the special winding structure of the dual-branch three-phase PMSM, the sum of the current harmonics in the two three-phase windings reflects the vibration noise of the motor. Once the carrier frequency and twice carrier frequency harmonics in the sum of three-phase current is reduced, the corresponding frequency vibration will be suppressed. As the harmonic component in the phase current varies as the modulation index, the results when the motor runs at different modulation ratios are demonstrated.

Fig. 7 shows the comparison results at low modulation ratio that motor speed is 240 r/min, and torque is 0.4 N • m. When the traditional method with no carrier phase-shift SVPWM is implemented, the harmonics at 8.0 kHz are larger than that at 4.0 kHz, and their amplitudes are greater than the other methods. It also can be observed that MSVPWM decreases the carrier frequency harmonics by 17.4 dBA and has almost no effect on the twice carrier frequency

harmonics. In contrast, the proposed method not only reduces the first carrier harmonics 16.4 dBA but also eliminates the second carrier harmonics to background noise. Similar results can be found in Fig. 8, wherein although all harmonic components are increased when the motor runs in the medium modulation ratio, the motor speed is 600 r/min, and the torque is 0.8 N • m. Here, the elimination effects the proposed method achieves are obvious.

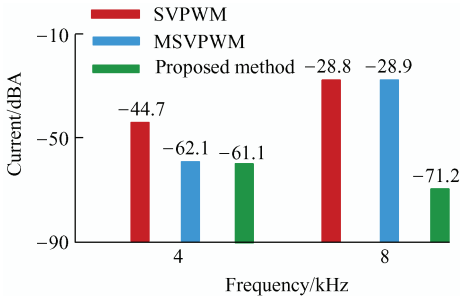

Fig. 7 Amplitude of carrier frequency and twice carrier frequency current harmonics with three methods when the motor runs at low modulation ratio

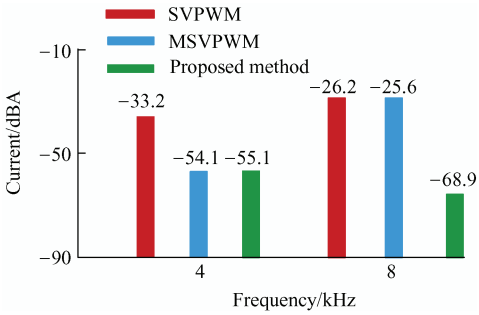

Fig. 8 Amplitude of carrier frequency and twice carrier frequency current harmonics with three methods when the motor runs at medium modulation ratio

The fast Flourier transform (FFT) spectrum of phase current sum with three methods at high modulation ratio that motor speed is 960 r/min and torque is 1.2 N • m can be seen in Fig. 9. MSVPWM reduces the carrier frequency harmonics, as analyzed in Section 3, which is not enough for noise reduction. The proposed method is able to reduce the carrier frequency harmonics by 18.2 dBA and eliminate the twice carrier frequency harmonics at the background level. Besides, the triple carrier frequency harmonics near 12.0 kHz is also reduced. However, the quadruple carrier frequency harmonics remain constant because the sum of the phase current in dual-branch three-phase PMSM is nonzero.

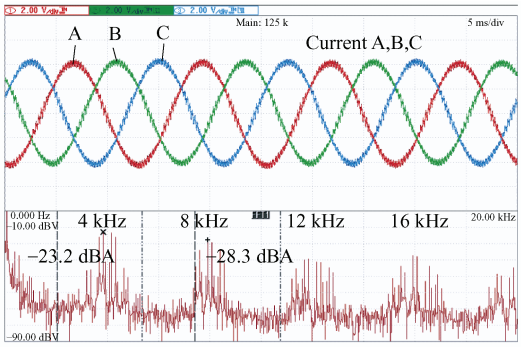

(a) Conventional SVPWM

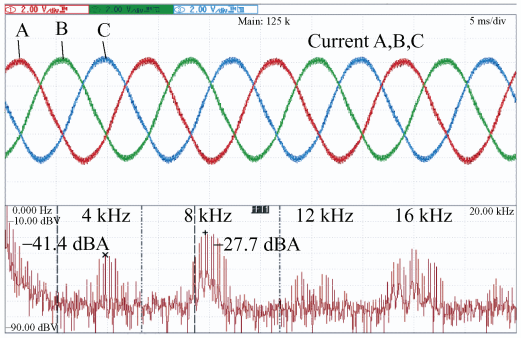

(b) MSVPWM

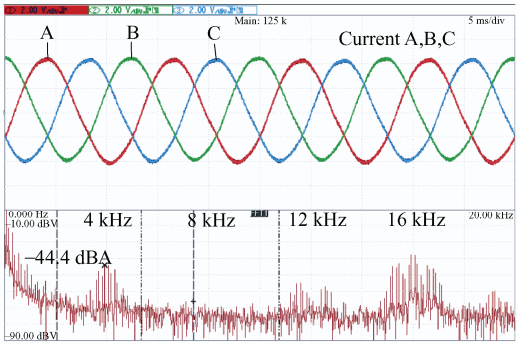

(c) Proposed method

Fig. 9 FFT results of carrier frequency and twice carrier frequency current harmonics when the motor runs at high modulation ratio

4.2 Results for PWM vibration harmonics reduction

As deduced in Section 3, the corresponding frequency vibration noise will therefore be suppressed after the reduction of current harmonics. Fig. 10 shows the comparison results when the motor runs at a low modulation ratio. Taking traditional SVPWM as the basic level, MSVPWM decreases the carrier frequency by 12.9 dBV. By comparison, the proposed method reduces the carrier frequency harmonics by 15.3 dBV and eliminates the twice carrier frequency harmonics completely. For medium modulation ratio in Fig. 11, the carrier frequency harmonics are decreased by 23.3 dBV, whereas twice carrier frequency harmonics are reduced by 58.3 dBV.

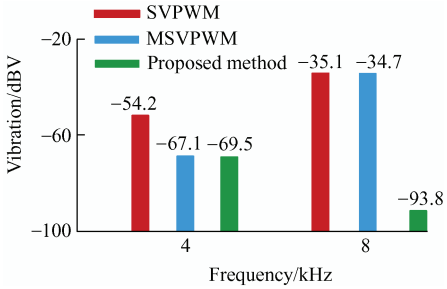

Fig. 10 Amplitude of carrier frequency and twice carrier frequency vibration harmonics with three methods when the motor runs at low modulation ratio

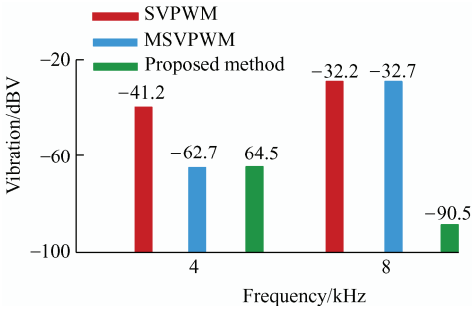

Fig. 11 Amplitude of carrier frequency and twice carrier frequency vibration harmonics with three methods when the motor runs at medium modulation ratio

The FFT spectrum of vibration signals with the three methods at a high modulation ratio can be seen in Fig. 12. As analyzed in Section 3, when MSVPWM suppresses the carrier frequency vibration harmonics, the vibration signal will be suppressed. In contrast, the proposed method reduces the carrier frequency

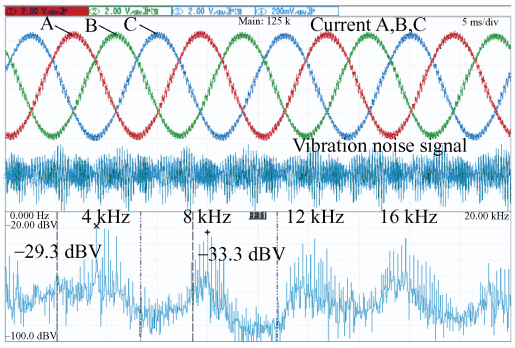

(a) Conventional SVPWM

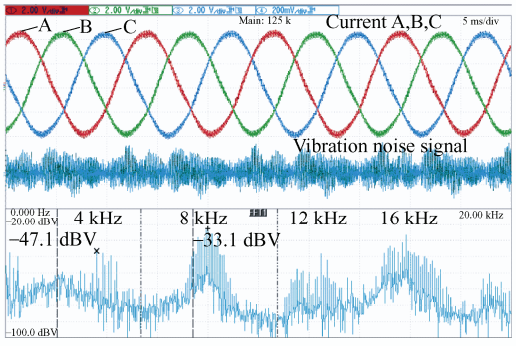

(b) MSVPWM

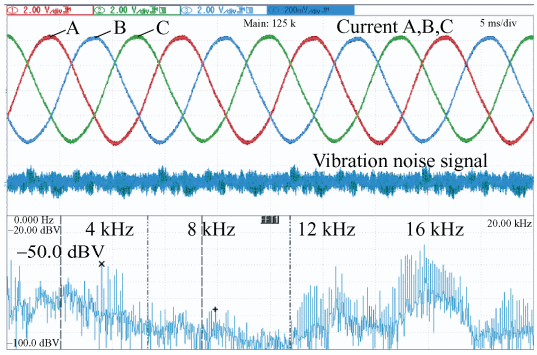

(c) Proposed method

Fig. 12 FFT results of carrier frequency and twice carrier frequency vibration harmonics when the motor runs at high modulation ratio

harmonics by 22.1 dBV and eliminates the twice carrier frequency harmonics.

4.3 Results for PWM acoustic noise reduction

It is well known that vibration is the source of sound. If the high-frequency vibration noise is reduced, the acoustic noise will therefore be suppressed.

Acoustic noise for low, medium, and high modulation ratios are all measured by a noise analyzer. Figs. 13 and 14 show the comparison results with three methods of noise reduction. Similarly, acoustic noise with MSVPWM at twice carrier frequency almost remains the same as SVPWM but eliminates the carrier frequency noise by 15.5 dBV and 21.2 dBV in Figs. 13 and 14, respectively. The proposed method achieves a reduction of carrier frequency noise of 16.2 dBV, and that of the twice carrier frequency noise by 35.4 dBV (for a low modulation ratio), compared with the traditional SVPWM. Further, it also has similar effects on the carrier frequency and twice carrier frequency noise for a medium modulation ratio.

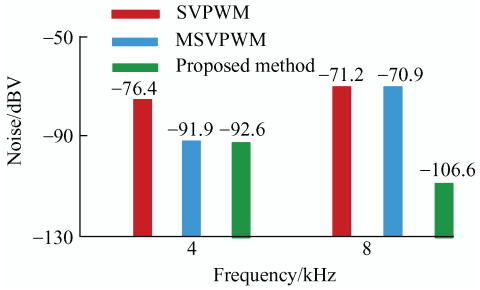

Fig. 13 Amplitude of carrier frequency and twice carrier frequency acoustic noise with three methods when the motor runs at low modulation ratio

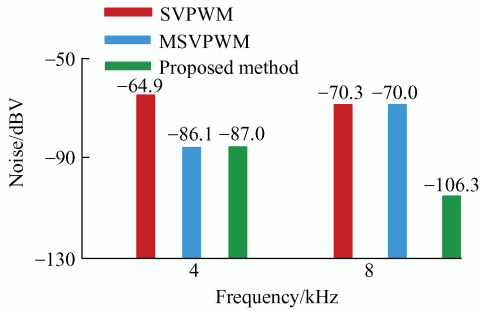

Fig. 14 Amplitude of carrier frequency and twice carrier frequency acoustic noise with three methods when the motor runs at medium modulation ratio

When motor runs in high modulation indices, from Fig. 15, the spectrum of the noise signal shows the effectiveness of the hybrid method. Compared with Figs. 15a and 15b, Fig. 15c demonstrates the noise reduction at the carrier frequency and twice carrier frequency, which is in accordance with the vibration spectrum. The motor is driven on a test bench, the noise caused by mechanical vibration is also received by the noise analyzer. Therefore, the amplitude of noise has not been obviously reduced.

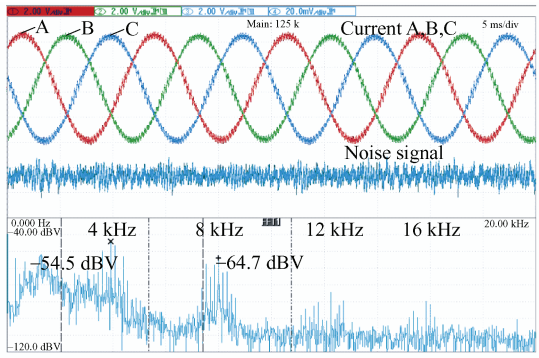

(a) Conventional SVPWM

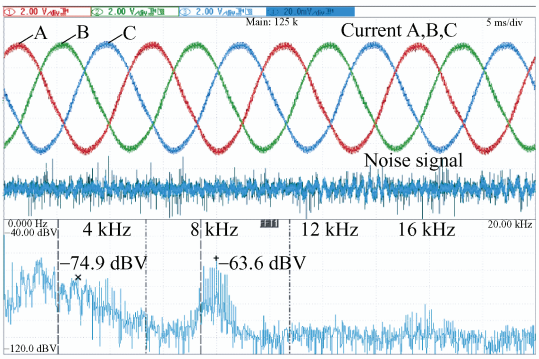

(b) MSVPWM

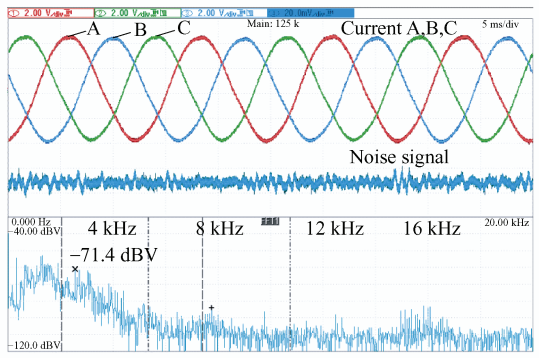

(c) Proposed method

Fig. 15 FFT results of first and second carrier frequency acoustic noise when the motor runs at high modulation ratio

5 Conclusions

This paper presents an effective method combining the carrier phase-shift technique and MSVPWM for branch three-phase PMSM, driven by paralleled VSIs with coupled inductors, to eliminate high-frequency PWM vibration.

The proposed method can reduce the carrier frequency harmonic current, thus suppressing the corresponding frequency vibration. Moreover, the proposed method maintains the sum of twice carrier frequency PWM harmonic current close to zero. Then, the MMF produced by the twice carrier frequency harmonics in the two three-phase windings are offset with each other, contributing to the elimination of the twice carrier frequency vibration.

The experimental results further verify the analysis of the vibration elimination principle. The high-frequency current harmonics, vibration, and acoustic noise are closely related to the motor. Irrespective of the modulation index, high-frequency vibration around the carrier frequency is reduced, and that around the twice carrier frequency is eliminated.

References

[1] C Liu, Y Luo. Overview of advanced control strategies for electric machines. *Chinese Journal of Electrical Engineering*, 2017, 3(2): 53-60.

[2] Y Demir, M Aydin. A novel asymmetric and unconventional stator winding configuration and placement for a dual three-phase surface PM motor. *IEEE Transactions on Magnetics*, 2017, 53(11): 1-5.

[3] E Levi. Multiphase electric machines for variable-speed applications. *IEEE Trans. Ind. Electron*, 2008, 55(5): 1893-1909.

[4] M Barcaro, N Bianchi, F Magnussen. Analysis and tests of a dual three-phase 12-slot 10-pole permanent-magnet motor. *IEEE Trans. Ind. Appl.*, 2010, 46(6): 2355-2362.

[5] X Han, D Jiang, T Zou, et al. Two-segment three-phase

PMSM drive with carrier phase-shift PWM for torque ripple and vibration reduction. *IEEE Trans*. *Power Electron*., 2018, 34(1): 588-599.

[6] J Karttunen, S Kallio, P Peltoniemi, et al. Dual three-phase permanent magnet synchronous machine supplied by two independent voltage source inverters. *Proc. Int. Symp. Power Electron., Elect. Drives, Autom. Motion*, 20-22 June, Sorrento, Italy. New York: IEEE, 2012: 741-747.

[7] W Liang, J Wang, P C K Luk, et al. Analytical modeling of current harmonic components in PMSM drive with voltage-source inverter by SVPWM technique. *IEEE Trans*. *Energy Convers*., 2014, 29(3): 673-680.

[8] K Chen, Z Zhao, L Yuan, et al. The impact of nonlinear junction capacitance on switching transient and its modeling for SiC MOSFET. *IEEE Trans*. *Electron Devices*, 2015, 62(2): 333-338.

[9] H Wang, A M H Kwan, Q Jiang, et al. A GaN pulse width modulation integrated circuit for GaN power converters. *IEEE Trans*. *Electron Devices*, 2015, 62(4): 1143-1149.

[10] Z Fang, D Jiang, Y Zhang. Study of the characteristics and suppression of EMI of inverter with SiC and Si devices. *Chinese Journal of Electrical Engineering*, 2018, 4(3): 37-45.

[11] S K T Miller, T Beechner, J Sun. A comprehensive study of harmonic cancellation effects in interleaved three-phase VSCs. *IEEE Power Electronics Specialists Conference*, 17-21 June, Orlando, Florida, IEEE, 2007.

[12] C Casablanca, J Sun. Interleaving and harmonic cancellation effects in modular three-phase voltage-sourced converters. *IEEE Workshops on Computers in Power Electronics*, Troy, NY, 2006: 275-281.

[13] D Zhang, F Wang, R Burgos, et al. Impact of interleaving on AC passive components of paralleled three-phase voltage-source converters. *IEEE Trans*. *Ind*. *Appl*., 2010, 46(3): 1042-1054.

[14] Y Miyama, M Ishizuka, H Kometani, et al. Vibration reduction by applying carrier phase-shift PWM on dual three-phase winding permanent magnet synchronous motor. *IEEE Trans*. *Ind*. *Appl*., 2018, 54(6): 5998-6004.

[15] Y Huang, Y Xu, W Zhang, et al. PWM frequency noise cancellation in two-segment three-phase motor using parallel interleaved inverters. *IEEE Trans*. *Power Electron*., 2019, 34(3): 2515-2525.

[16] W Zhang, Y Xu, H Huang, et al. Vibration reduction for dual-branch three-phase permanent magnet synchronous motor with carrier phase-shift technique. *IEEE Trans*. *Power Electron*., 2020, 35(1): 607-618.

[17] R L Kirlin, M M Bech, A M Trzynadlowski. Analysis of power and power spectral density in PWM inverters with randomized switching frequency. *IEEE Trans*. *Ind*. *Electron*., 2002, 49(2): 486-499.

[18] M M Bech, F Blaabjerg, J K Pedersen. Random modulation techniques with fixed switching frequency for three-phase power converters. *IEEE Trans*. *Power Electron*., 2000, 15(4): 753-761.

[19] K Lee, G Shen, W Yao, et al. Performance characterization of random pulse width modulation algorithms in industrial and commercial adjustable-speed drives. *IEEE Trans*. *Ind*. *Appl*., 2017, 53(2): 1078-1087.

[20] Y Huang, Y Xu, Y Li, et al. PWM frequency voltage noise cancelation in three-phase VSI using the novel SVPWM strategy. *IEEE Trans*. *Power Electron*., 2018, 33(10): 8596-8606.

[21] Y Huang, Y Xu, W Zhang, et al. Hybrid RPWM technique based on modified SVPWM to reduce the PWM acoustic noise. *IEEE Trans*. *Power Electron*., 2019, 34(6): 5667-5674.

[22] G Gohil, L Bede, R Teodorescu, et al. An integrated inductor for parallel interleaved three-phase voltage source converters. *IEEE Trans*. *Power Electron*., 2016, 31(5): 3400-3414.

[23] D Zhang, F Wang, R Burgos, et al. Total flux minimization control for integrated inter-phase inductors in paralleled, interleaved three-phase two-level voltage-source converters with discontinuous space-vector modulation. *IEEE Trans*. *Power Electron*., 2012, 27(4): 1679-1688.

[24] D G Holmes, T A Lipo. Pulse width modulation for power converters (principles and practice). Piscataway, NJ: IEEE Press, 2003.

[25] Y Huang, Y Xu, W Zhang, et al. Modified single-edge SVPWM technique to reduce the switching losses and increase PWM harmonics frequency for three-phase VSIs. *IEEE Trans*. *Power Electron*., DOI:10.1109/TPEL.2020.2975626.

[26] F Lin, S Zuo, W Deng, et al. Modeling and analysis of electromagnetic force, vibration, and noise in permanentmagnet synchronous motor considering current harmonics. *IEEE Trans*. *Ind*. *Electron*., 2016, 63(12): 7455-7466.

[27] Z Q Zhu, Z P Xia, L J Wu, et al. Analytical modeling and

finite-element computation of radial vibration force in fractional-slot permanent-magnet brushless machines. *IEEE Trans*. *Ind*. *Appl*., 2010, 46(5): 1908-1918.

Wentao Zhang received a B.S. degree in electrical engineering and automation from Harbin Institute of Technology, Weihai, China, in 2016. He is currently working toward a Ph.D. degree at Harbin Institute of Technology, Harbin, China.

His research interests include PMSM drives and control algorithms.

Yongxiang Xu (M'03) was born in Guangxi Province, China, in 1977. He received M.S. and Ph.D. degrees in electrical engineering from Harbin Institute of Technology, Harbin, China, in 2001 and 2005, respectively.

He is currently a professor in School of Electrical Engineering and Automation, Harbin Institute of Technology. His current research interests include permanent-magnet machine design and control.

Yingliang Huang was born in Inner Mongolia, China, in 1990. He received the M.S. and Ph.D. degrees in electrical engineering from Harbin Institute of Technology, Harbin, China, in 2015 and 2019, respectively.

He is currently a chief engineer in Automotive Products Group, Johnson Electric, Shenzhen, China. His current research interests include power converter and permanent-magnet motor drives.

Jibin Zou (SM'00) was born in Heilongjiang Province, China, in 1957. He received the M.S. and Ph.D. degrees in electrical engineering from Harbin Institute of Technology, Harbin, China, in 1984 and 1988, respectively.

Since 1985, he has been engaged in the research in electrical machines. He was working with the University of Liverpool, Liverpool, UK, as a visiting research fellow for one year. He is now a professor in the State Key Laboratory of Robotics and System, Harbin Institute of Technology. Prof. Zou is a senior member of the IEEE Magnetics society since 2000. His current research interests include permanent-magnet machine design and control.